Bioorganic Chemistry 40 (2012) 108–113

Contents lists available at SciVerse ScienceDirect

Bioorganic Chemistry

journal homepage: www.elsevier.com/locate/bioorg

A water soluble tri-cationic porphyrin–EDTA conjugate induces apoptosis in human neuroendocrine tumor cell lines

Gert Schwach [a], Patchanita Thamyongkit [b], Lorenz Michael Reith [c], Bernhard Svejda [a], Günther Knör [c], Roswitha Pfragner [a,*], Wolfgang Schoefberger [c,*]

[a] Department of Pathophysiology and Immunology, Center of Molecular Medicine, Medical University of Graz, A-8010 Graz, Austria
[b] Department of Chemistry, Faculty of Science, Chulalongkorn University, Phayathai Road, Patumwan, Bangkok 10330, Thailand
[c] Institute of Inorganic Chemistry, Johannes Kepler University Linz (JKU), Altenberger Straße 69, 4040 Linz, Austria

ARTICLE INFO

Article history:
Received 12 September 2011
Available online 6 October 2011

Keywords:
Cationic porphyrin
Chelator
Antitumor agent
Human neuroendocrine tumor cells
Medullary thyroid carcinoma cell lines
Small intestinal carcinoma cell lines

ABSTRACT

In this study, a completely water soluble tri-cationic porphyrin–EDTA conjugate was synthesized. We present data demonstrating the tumoristatic effects of the novel fully water soluble cationic porphyrin $TMPy_3PhenEDTA\text{-}P\text{-}Cl_4$ in the dark, in the medullary thyroid carcinoma cell lines *MTC-SK* and *SHER-I* and weaker effects in the small intestinal neuroendocrine tumor cell line *KRJ-I*. In addition, cytotoxic effects were also studied in normal human fibroblasts that represent normal tissue and the results are compared to the tumor cell lines.

1. Introduction

Cationic porphyrins represent an expanding class of compounds, which have several applications in biology, medicine and catalysis and have been studied from the viewpoint of their role as DNA cleavers [1–5]. Recent studies about the interaction of cationic porphyrins and their derivatives with DNA have moved porphyrin compounds into the spotlight of an alternative anticancer strategy [3,6,7].

Small intestinal neuroendocrine tumors (SI-NETs) represent a group of rare neoplasms that are derived from enterochromaffin cells (ECs) [8–10]. Response rates to standard chemotherapy and radiotherapy are low and surgery remains the only curative treatment [11]. However, 60–80% of patients show metastases at the time of diagnosis and curative surgery is only performed in <15% of the cases [12].

Medullary thyroid carcinoma (MTC) is a neuroendocrine tumor arising from the parafollicular C-Cells of the thyroid gland and 25% of patients show distant metastases at the time of diagnosis [13–15].

Since both tumor types are known for their poor response to standard chemotherapy and radiotherapy, there is a substantial need for establishing new therapeutic strategies.

In this work we present the synthesis of a fully water soluble cationic porphyrin $TMPy_3PhenEDTA\text{-}P\text{-}Cl_4$ (Por-EDTA) **4** (Scheme 1), functionalized with an ethylene-diamintetraacetic acid EDTA moiety, a typical chelator for Fe or Cu ions [16].

The presence of Fe in ribonucleotide reductase is vital for proliferation owing to its role in catalyzing the rate-limiting step of DNA synthesis (i.e. the conversion of ribonucleotides into deoxyribonucleotides). The importance of Fe is highlighted by the fact that Fe deprivation leads to G_1-S arrest and apoptosis [17]. Neoplastic cells, in particular, have a high Fe requirement due to their rapid proliferation. To attain more Fe, neoplastic cells express higher levels of the transferrin receptor 1 (TfR1) and take up Fe more rapidly than their normal counterparts. This is reflected by the ability of tumors to be radiolocalized using ^{67}Ga, which binds to the Fe transport protein, transferrin, for delivery via TfR1 [18]. Similarly, phosphoro-thiolated antisense TfR1 oligonucleotides targeted to TfR1 mRNA showed selective anticancer activity [19], confirming the importance of Fe in cancer cell growth. These observations show how Fe chelation maybe a suitable therapeutic strategy for cancer treatment. In addition to Fe, Cu is also a promising therapeutic target due to its key role in angiogenesis [20]. Chelation of Cu suppresses several angiogenic mediators, including vascular endothelial growth factor-1, fibroblast growth factor-1, interleukin (IL)-1, IL-6, IL-8, and nuclear factor-κB [21]. Because angiogenesis is critical for tumor metastasis

* Corresponding authors. Address: Medical University Graz, Institute of Pathophysiology and Immunology, Heinrichstraße 31a, 8010 Graz, Austria (R. Pfragner).
E-mail addresses: roswitha.pfragner@medunigraz.at (R. Pfragner), wolfgang.schoefberger@jku.at (W. Schoefberger).

0045-2068
doi:10.1016/j.bioorg.2011.09.006

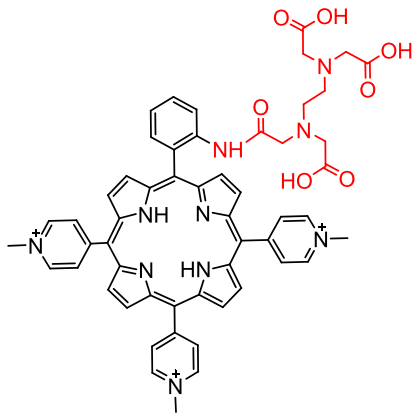

Scheme 1. Chemical structure of $TMPy_3PhenEDTA\text{-}P\text{-}Cl_4$ **4**.

[20], the ability of Cu chelators to inhibit angiogenesis represents a novel therapeutic strategy for cancer chemotherapy.

We herein show the antiproliferative effects of a completely water soluble cationic porphyrin–EDTA hybrid derivative **4** in the small intestinal neuroendocrine tumor (SI-NET) cell line *KRJ-I* [22], the medullary thyroid carcinoma (MTC) cell line *MTC-SK* [23], *SHER-I* [24] and the human fibroblast cell line *HF-SAR* [25].

2. Experiments

2.1. Materials and methods

All chemical reactions were carried out under nitrogen in degassed solvents, which were dried using conventional methods. Preparative thin layer chromatography was carried out on silica gel 60 F254 (Merck) 0.2 mm plates. The porphyrin precursors were visualized by UV–visible absorption (245–365 nm). Flash column chromatography was carried out using silica gel 60 (Merck) 230–400 mesh and distilled solvents. Pyrrole was freshly distilled before use. Other chemicals were purchased as reagent grade and applied without further purification.

2.2. Instruments

NMR spectra were recorded on a Bruker DRX NMR spectrometer equipped with a cryogenically cooled probe operating at 500 MHz for ^1H and 125.725 MHz for ^{13}C. ^1H chemical shifts and ^{13}C chemical shifts are reported relative to tetramethylsilane (TMS) and were reported as δ (ppm). Mass spectra were collected on a Finnigan LCQ DecaXPplus Ion trap Mass spectrometer with ESI ion source and an Agilent ESI-Q-TOF 6250. Porphyrin samples were dissolved in chloroform/methanol (1:1) or methanol and were

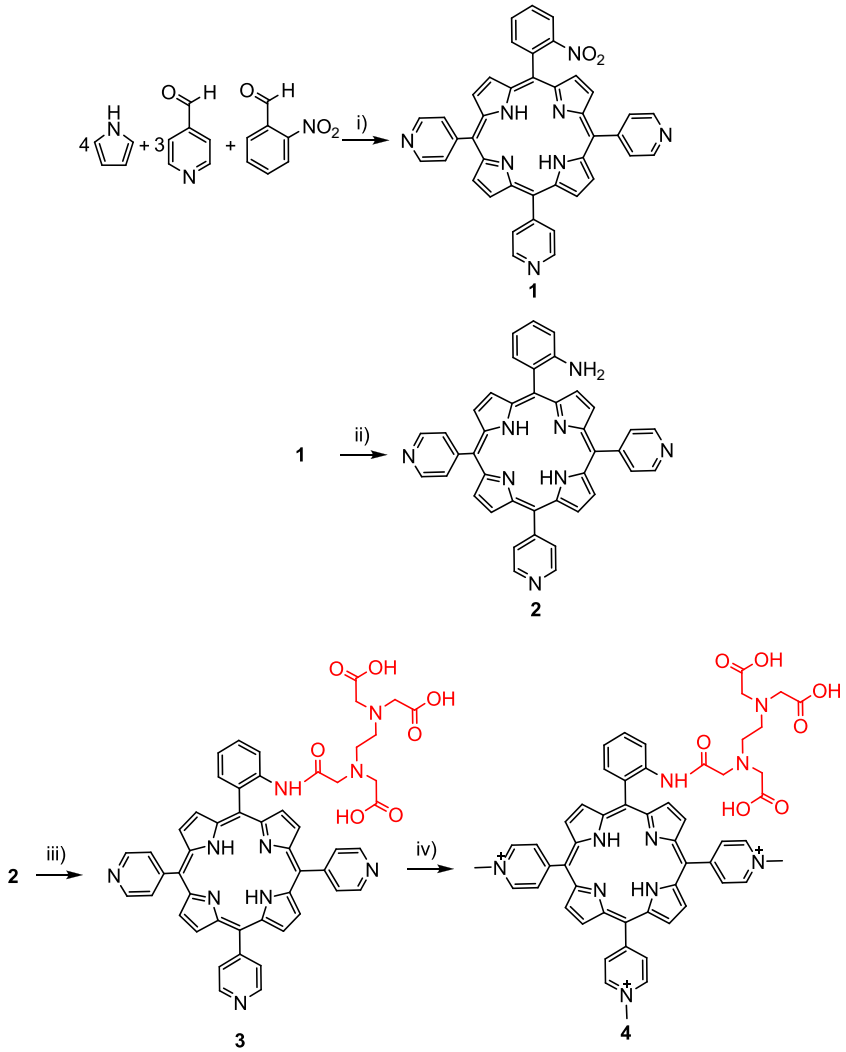

Scheme 2. Reaction scheme to obtain $TMPy_3PhenEDTA\text{-}P\text{-}Cl_4$ **4** and reaction conditions to obtain compound **4**: (i) Propionic acid/propionic anhydride, 1.5 mmol 2-nitrobenzaldehyde, 4.5 mmol 4-pyridine-carboxaldehyde refluxed (120 min), (ii) reduction with $SnCl_2$ in HCl, (iii) amidation with EDTA-di-anhydride in DMSO and TEA. Extensive Column Chromatography and HPLC were applied to purify the reaction products.

introduced to the mass spectrometer via infusion at a flow rate of 0.30 ml/h. The source and desolvation temperatures were 80 and 120 °C, respectively with a capillary voltage of 3.1 kV, sampling cone voltage of 58 V, and the extractor cone to 3 V. The collision energy was set to 14 eV and Argon was used as collision gas for the CID experiments, which was adjusted to a pressure of 1.7×10^{-4} mbar. UV-absorption spectra of porphyrins were carried out on a Varian CARY 100 Bio UV/visible-spectrometer equipped with Cary Temperature Controller (5 mM NaCacodylate, 20 mM NaCl, pH 7.0 buffer).

2.3. Synthesis of porphyrin precursors **1**, **2** and **3**

The starting 5-(2-nitrophenyl)-10,15,20-tris(4-pyridyl)-porphyrin [TMPyPhenNO_2P]Cl_3 **1** was obtained via two-step synthesis with the mixed aldehyde reaction of pyrrole, pyridine-4-carbaldehyd [26]. This reaction gave the desired mononitroporphyrin in an acceptable yield (12%). The subsequent reduction of the nitro group into the amino group was carried out in a mixture of hydrochloric acid in the presence of an excess (12 equivalents) of $SnCl_2 \cdot 2H_2O$, while protecting the reaction mixture from the light. The final 5-(4-aminophenyl)-10,15,20-tris(4-pyridyl)-porphyrin [TMPyPhenNH_2P]Cl_3 **2** was obtained in 80% yield. The synthetic scheme to obtain the Por-EDTA hybrids is shown in Scheme 2.

2.4. Synthesis of Por-EDTA hybrid **4** (5,10,15-tris(N-methylpyridinium-4-yl)-20-(1-phenyl-2-(ethylene diamine-tetra acetic acid))-21H,23H-porphyrin)

A mixture of 0.474 mmol $TPy_3(PhenNH_2)_1P$ **2** and 0.569 mmol ethylenediaminetetraacetic acid dianhydride in dimethylsulfoxide and triethylamine was stirred for 30 min under inert gas. Subsequently, water was added and compound **3** was extracted with dichloromethane (DCM) and little amount of sodium chloride was added to enhance the solubility in DCM. Purification was performed with column chromatography ($CHCl_3$/hexane 1:1) and product **3** was isolated in 90% yield. Step two was immediately performed after work up, where to a mixture of 10 ml CH_3NO_2 and 10 ml $CHCl_3$ (1:1 v/v) 0.2 mmol $TPy_3PhenEDTA_1P$ **3** and 1.1 mmol methyliodide were added. This reaction mixture was refluxed for 90 h under argon atmosphere. The progress of the N-methylation reaction can be monitored using silica gel TLC and an eluent containing ACN:H_2O (sat. KNO_3):H_2O 8:1:1 (v/v). Then the reaction mixture was evaporated to dryness, dissolved in deionized water and the impurities were extracted with $CHCl_3$.

Compound **4** was then flushed through an amberlite (A-21) Cl^- ion exchange resin and purified with reversed phase HPLC (eluent mixture: ACN/MeOH = 50/1).

The remaining ACN/MeOH fraction was then evaporated to dryness which gave the chloride salt of $TMPy_3PhenEDTA_1P\text{-}Cl_3$ **4** in 90% yields.

^1H NMR (500 MHz, D_2O, 303.57 K, δ [ppm]): 8.93 (d, J = 5.83 Hz, 6H, pyridyl-3,5-H), 8.85 (d, J = 4.1 Hz, 2H, β-pyrrole-H), 8.55 (d, J = 4.1 Hz, 2H, β-pyrrole-H), 8.29 (d, J = 5.83, 6H, pyridyl-2,6-H), 8.19 (d, J = 4.1 Hz, 2H, β-pyrrole-H), 7.76 (d, J = 4.1 Hz, 2H, β-pyrrole-H) 6.95–6.85 (m, 4H, phenyl-H), 4.39 (s, 9H, N^+–CH_3), 2.59 (br, m, 12H, –CH_2–).

^{13}C NMR (125 MHz, D_2O, 303.57 K, δ [ppm]): 177.1 (q, –COOH), 168.4 (q, –NHCO–), 153.0 (q, pyridyl-1-*C*), 149.0 (pyridyl-*CH*), 147.7 (β-pyrrole-*CH*), 146.6 (β-pyrrole-*CH*), 129.7 (β-pyrrole-*CH*), 129.1 (pyridyl-*CH*), 128.7 (β-pyrrole-CH), 137.2 (q, phenyl-*C*), 124.4 (phenyl-*CHs*), 51.3 (–N^+–CH_3), 36,4 (–CH_2–) (q – quaternary carbon).

ESI-MS (**4** in $CHCl_3$: MeOH (1:1), positive ion mode): m/z = 317.23 ($[M]^{3+}$), 475.71 ($[M]^{2+}$), theoretical mass = 951.39 (Sum formular = $C_{54}H_{51}N_{10}O_7$).

UV–Vis (**4** in aqueous buffer solution containing 5 mM NaCacodylate, 20 mM NaCl, pH 7.0): λ_{max} (nm) ($\log \varepsilon$) = 421.3 nm (4.92), 512.6 (3.31), 547.4 (3.16), 589.4 (3.05).

2.5. Cell culture conditions

MTC-SK, *SHER-I* and *KRJ-I* cells were cultured in Ham's F12/M199 (1:1) (Biowhittaker, Verviers, Belgium) supplemented with 10% FBS (PAA Laboratories, Pasching, Austria). *HF-SAR* cells were maintained in Eagle's minimal essential medium (Biowhittaker, Verviers, Belgium) containing 10% FBS All cell lines were *Mycoplasma* free and maintained without antibiotics at 37 °C and 5% CO_2.

2.6. Cell counting

MTC-SK, *SHER-I* and *KRJ-I* cells were incubated in 24 well plates (2×10^5 cells/ml) and treated with different concentrations of Por-EDTA for 24, 48 and 72 h, Aqua bidest was used as negative control. Cell counts were performed using CASY®-1 Cell Counter & Analyzer TTC (Schärfe System, Reutlingen, Germany). Each sample was quantified three times.

2.7. WST-1 cell proliferation assay

MTC-SK, *SHER-I*, *KRJ-I* and *HF-SAR* cells were seeded in 24 well plates (2×10^5 cells/ml) and treated with different concentrations of porphyrin **4** for 24, 48 and 72 h. After incubation the cells were

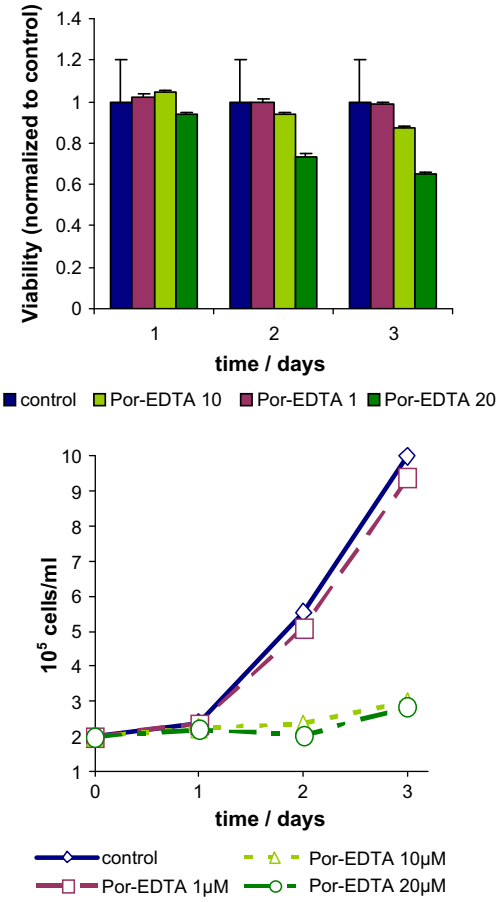

Fig. 1. Cytotoxic effects of different concentrations (1, 10 and 20 µM) of $TMPy_3PhenEDTA\text{-}P\text{-}Cl_4$ **4** in MTC cell lines: effects of $TMPy_3PhenEDTA\text{-}P\text{-}Cl_4$ **4** on cell viability quantified using WST-1 assay. Comparison of antiproliferative activity of $TMPy_3PhenEDTA\text{-}P\text{-}Cl_4$ **4**: a decrease in counted cells was noted in *MTC-SK* cells compared to untreated control.

carefully pipetted to obtain single cells. One-hundred microliters cell suspension was transferred into a 96 well plate. After adding 10 µl of WST-1 reagent an additional incubation of 2 h at 37 °C and 5% CO_2 was performed. Then the samples were analyzed spectrophotometrically by measuring the absorbance at 450 nm using an ELISA plate reader (Molecular Devices Thermomax Plate Reader, Pegasus Scientific Inc., Rockville, USA). The adherent cell line *HF-SAR* was seeded directly into the 96 well plates at a density of 1×10^5 cells/ml. After adherence to the plates the cells were treated with porphyrin **4** and viability was measured at 24, 48 and 72 h as described above. Values of each sample ($n = 6$) were averaged and normalized to control.

2.8. Hoechst 33258 staining

Hoechst stain solution (Bisbenzimide H33258) H6024 (Sigma–Aldrich); MTC-SK cells were seeded in 6 well plates (Sarsted, Wr Neudorf, Austria) (2×10^5 cells/ml) and treated with 10 µM Por-EDTA for 48 h. Thereafter the cell suspensions were centrifuged at 300 g, the supernatant removed and cell pellet washed with Hoechst 33258:PBS (1:50) and incubated 15 min at 37 °C. After a new centrifugation at 300 g cells were resuspended in PBS and examined using a LEICA DM 4000B microscope with ultraviolet excitation at 300–500 nm (Leica EL 6000 BZ01).

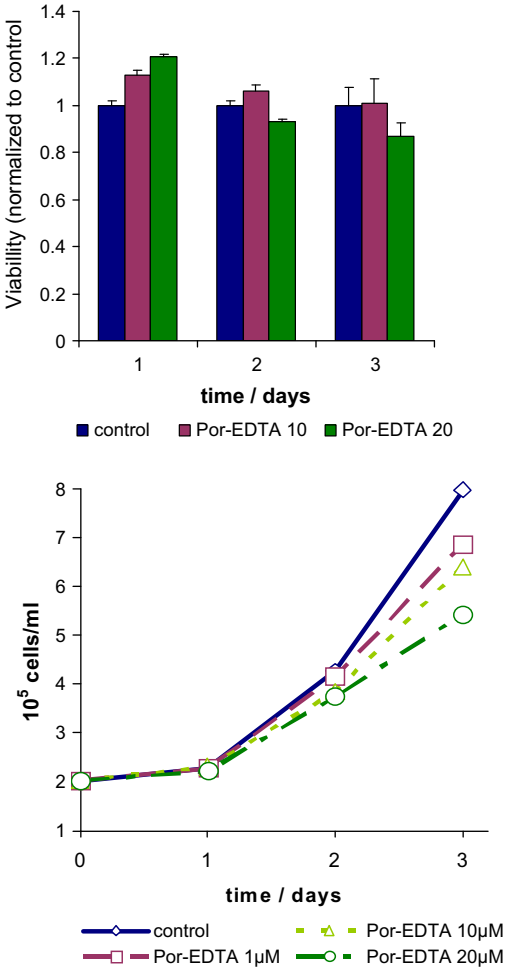

Fig. 2. Cytotoxic effects of different concentrations (1, 10 and 20 µM) of $TMPy_3PhenEDTA\text{-}P\text{-}Cl_4$ **4** in *KRJ-I* cell line: effects of $TMPy_3PhenEDTA\text{-}P\text{-}Cl_4$ **4** on cell viability quantified using WST-1 assay. Only a small concentration dependent decrease in counted cells was noted in *KRJ-I* cells compared to control. (For interpretation of the references to colour in this figure legend, the reader is referred to the web version of this article.)

2.9. Assessment of caspase-3/7 activity

MTC-SK cells were plated in 96-well plates and treated with porphyrin **4** (5 µM and 10 µM) up to 72 h or left untreated. Caspase-Glo® 3/7 Reagent and Rhodamine-110 Substrate were added to wells, and luminescence and fluorescence were recorded starting at one hour. Luminescence was recorded on a Dynex MLX® luminometer and fluorescence was recorded on a LabSystems Fluoroscan Ascent fluorimeter (485Ex/527Em). Results were plotted as signal-to-noise ratios. Background readings were determined from wells containing culture medium without cells.

3. Results and discussion

3.1. Cell survival assays

It is an essential prerequisite to understand the mechanism of inhibition of tumor cells to develop anticancer drugs based on cationic porphyrinoid systems. Recently, the tumor inhibition mode of cationic porphyrin was described as down regulation of *c-MYC* and human telomerase reverse transcriptase expression [6].

To verify and quantify the inhibition of tumor cell growth after incubation with porphyrin **4**, we first applied WST-1 cell proliferation assays *in vitro* in medullary thyroid carcinoma cells and small intestinal neuroendocrine tumor cells [3]. Cytotoxic data were expressed as IC_{50} values (the concentration of the test agent inducing 50% reduction in cell numbers compared with control cultures),

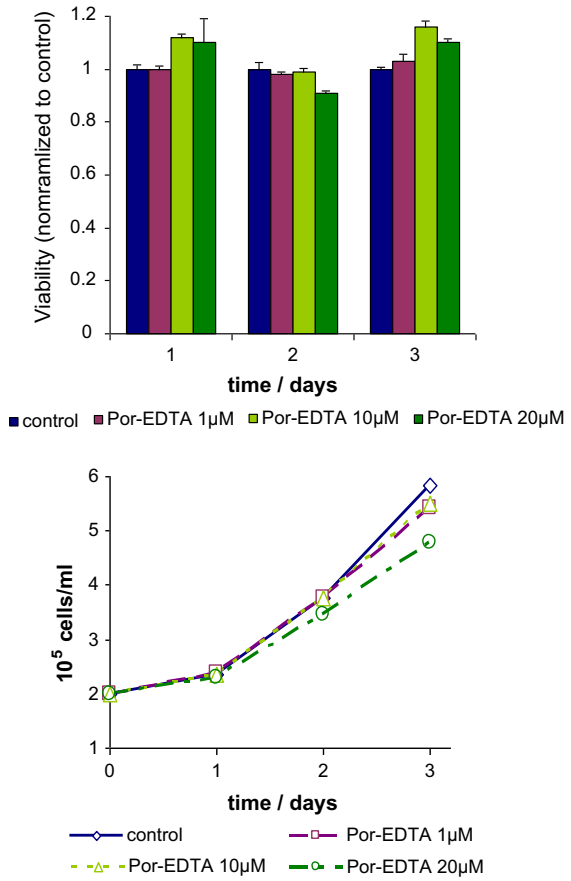

Fig. 3. Cytotoxic effects of different concentrations (1, 10 and 20 µM) of $TMPy_3PhenEDTA\text{-}P\text{-}Cl_4$ **4** in human *SHER-I* cell line: effects of $TMPy_3PhenEDTA\text{-}P\text{-}Cl_4$ **4** on cell viability quantified using WST-1 assay and Casy-1® Cell Counter analyses. (For interpretation of the references to colour in this figure legend, the reader is referred to the web version of this article.)

and the corresponding IC_{50} values are 5.1 μM for MTC-SK, 9.3 μM for SHER-I and 37.2 μM for KRJ-I.

Additionally, cell counting confirmed results found by the WST-1 studies. In *MTC-SK* cells and *SHER-I* cells porphyrin **4** had a high

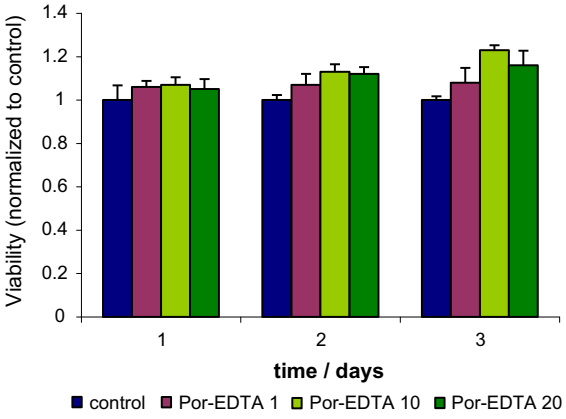

Fig. 4. Cytotoxic effects of different concentrations (1, 10 and 20 μM) of $TMPy_3PhenEDTA\text{-}P\text{-}Cl_4$ **4** in human fibroblast cell line *HF-SAR*: effects of $TMPy_3PhenEDTA\text{-}P\text{-}Cl_4$ **4** on cell viability quantified using WST-1 assay and Casy-1® Cell Counter analyses. (For interpretation of the references to colour in this figure legend, the reader is referred to the web version of this article.)

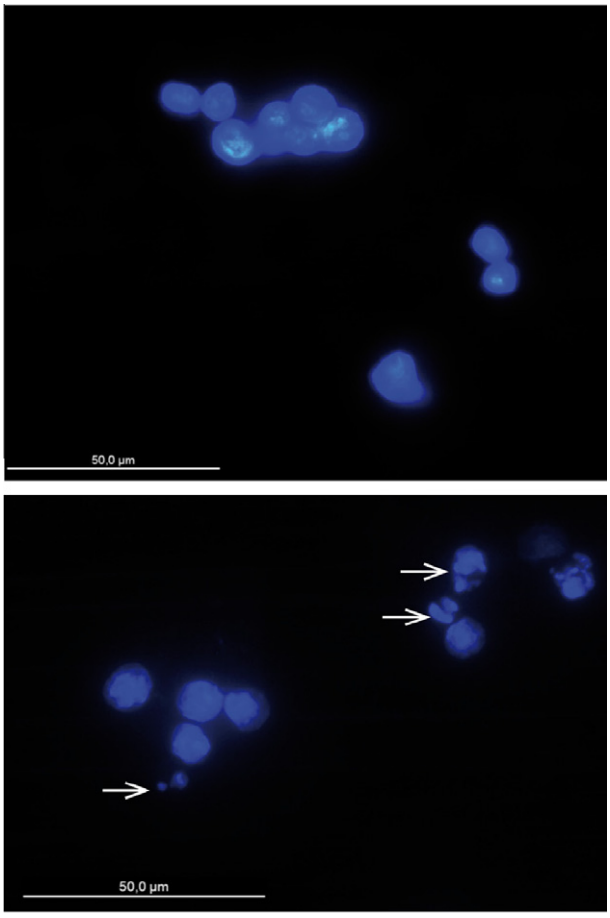

Fig. 5. Incubation of *MTC-SK* cells with TMPy3PhenEDTA-P-Cl_4 **4**. Nuclear staining was performed using Hoechst 33258 (DAPI) dye. While no morphological changes were evident in the control. Nuclear body fragments and irregular edges around the nucleus were observed (white arrows), 10 μM $TMPy_3PhenEDTA\text{-}P\text{-}Cl_4$ **4**.

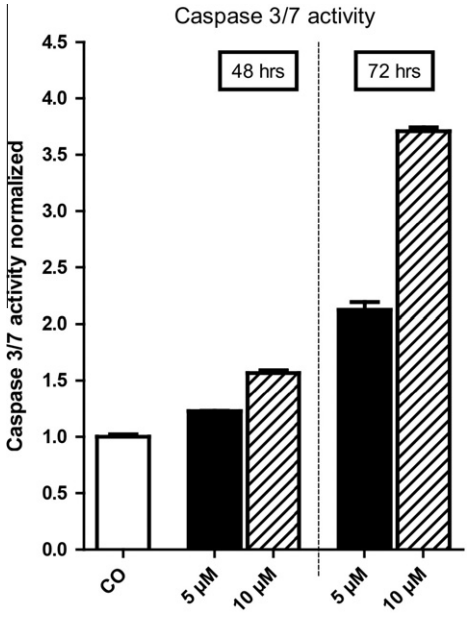

Fig. 6. Normalized effector caspase 3/7 activity after 48 and 72 h in *MTC-SK* cells.

antiproliferative effect (Figs. 1 and 2), while cell proliferation data of *KRJ-I* cells showed low values of growth inhibition (Fig. 3).

To further investigate effects of the novel porphyrin compound **4**, WST-1 tests on normal tissue were performed. The cell viability of *HF-SAR* cells treated with **4** was even higher compared to the untreated control (see Fig. 4). Comparing the effects of porphyrin **4** in the tumor cell lines and fibroblast cell line, a constant decrease of cell viability was noted in tumor cells, while, after an initial decrease in cell viability, fibroblasts were not significantly altered. Using light microscopy an increase in cell debris and dead cells was observed in tumor cell lines, while no significant effect was noted in fibroblasts compared to the untreated control. These findings suggest a different mechanism in normal cells compared to tumor cells.

3.2. Apoptosis of MTC-cells

We selected first the *MTC* cells as our model system to carry out investigations to elucidate the underlying intracellular signalling pathway leading to the terminal cell death.

At first, to identify if necrosis or apoptosis occurs in the tumor cells, the morphology of cells was investigated by staining with Hoechst 33258, a blue fluorescent DNA dye. After performing this standard staining protocol on the non-treated and treated *MTC*-cells, the morphological changes such as chromatin condensation, nuclear pyknosis and increased number of nuclear body fragments became evident (Fig. 5B, marked with arrows). This morphology features point to apoptosis as the predominant cell death process.

To confirm this assumption we performed the caspase-Glo® 3/7 assay which is a luminescent assay that measures caspase-3 and -7 activities. Indeed, we investigated high caspase 3/7 activity after 48 and 72 hours after incubation with porphyrin **4** (Fig. 6).

4. Conclusion

To conclude, our findings demonstrate a significant antiproliferative effect of the novel water soluble tri-cationic porphyrin/EDTA hybrid **4** in MTC cell line *MTC-SK*, while normal tissue was not significantly impaired.

The porphyrin **4** demonstrates a dose-dependent decrease in mitochondrial activity in MTC (*MTC-SK and SHER-I* cell lines) with IC_{50}s of 5.1 μM and 9.3 μM, respectively. The tumoristatic effects were accompanied by reduced cell proliferation quantified by a Casy-1® Cell Counter and Analyser. Based on these findings we conclude that EDTA modified porphyrins demonstrate high cytotoxicity towards the investigated tumor cell lines. Of particular interest is that no mitochondrial activity alterations were noted in the fibroblast derived cell line *HF-SAR* suggesting antiproliferative specificity for tumor cells. Previous studies described a specific accumulation of photo-sensitizers in tumor tissue with less compound enhancement in normal tissue. We hypothesize that a similar effect could be responsible for the continuous decrease in tumor cell viability, while fibroblasts were only impaired initially and showed no constant inhibition of cell proliferation.

Moreover, all experimental data supported the fact that such porphyrin had good abilities to induce apoptosis preferably on medullary thyroid carcinoma cell lines (*MTC-SK*) even in the dark and thus, might be a new therapeutic option in treatment of chemo-resistant neuroendocrine tumors. Different effects were observed in *KRJ-I* cells, where low tumoristatic effects were found.

Ongoing work focuses on the evaluation of how light exposure alters the tumoristatic effects in the Por-EDTA **4**/neuroendocrine tumor cell line system.

Acknowledgments

W.S. and R.P. acknowledge the support by the Austrian Science Fund FWF (P-18384-Solid state and liquid NMR of biomolecular metalcomplexes, to W.S.), by Stadt Graz Wissenschaft and the Franz Lanyar Foundation. W.S. also acknowledges the help of Dr. Klaus Wolkenstein and Dr. Clemens Schwarzinger for ESI-Q-TOF MS and MALDI-TOF MS measurements. We thank Veronika Siegl for excellent technical assistance.

References

[1] U. Sehlstedt, S.K. Kim, P. Carter, J. Goodisman, J.F. Vollano, B. Norden, J.C. Dabrowiak, Biochemistry 33 (1994) 417.
[2] G. Pratviel, J. Bernadou, M. Ricci, B. Meunier, Biochem. Biophys. Res. Commun. 160 (1989) 1212.
[3] M. Haeubl, S. Schuerz, B. Svejda, L.M. Reith, B. Gruber, R. Pfragner, W. Schoefberger, Eur. J. Med. Chem. 45 (2010) 760.
[4] G. Pratviel, M. Pitie, J. Bernadou, B. Meunier, Nucleic Acids Res. 19 (1991) 6283.
[5] M. Haeubl, L.M. Reith, B. Gruber, U. Karner, N. Müller, G. Knör, W.J. Schoefberger, Biol. Inorg. Chem. 14 (2009) 1037.
[6] C.L. Grand, H. Han, R.M. Munoz, S. Weitman, D.D.V. Hoff, L.H. Hurley, D.J. Bearss, Mol. Cancer Ther. 1 (2002) 565.
[7] D.P.N. Gonçalves, S. Ladame, S. Balasubramanian, J.K.M. Sanders, Org. Biomol. Chem. 4 (2006) 3337.
[8] I.M. Modlin, K. Oberg, D.C. Chung, R.T. Jensen, W.W. Herder, R.V. Thakker, M. Caplin, G.D. Fave, G.A. Kaltsas, E.P. Krenning, S.F. Moss, O. Nilsson, G. Rindi, R. Salazar, P. Ruszniewski, A. Sundin, Lancet Oncol. 9 (2008) 61.
[9] R. Toni, J. Endocrinol. Invest. 27 (2004) 35.
[10] I.M. Modlin, K.D. Lye, M. Kidd, Cancer 97 (2003) 934.
[11] I.M. Modlin, M. Kidd, I. Latich, M.N. Zikusoka, M.D. Shapiro, Gastroenterology 128 (2005) 1717.
[12] I.M. Modlin, I. Latich, M. Kidd, M. Zikusoka, G. Eick, Clin. Gastroenterol. Hepatol. 4 (2006) 526.
[13] A.O. Hoff, P.M. Hoff, Hematol. Oncol. Clin. North Am. 21 (2007) 475.
[14] C. Jimenez, M.I. Hu, R.F. Gagel, Endocrinol. Metab. Clin. North Am. 37 (2008) 481.
[15] R.M. Tuttle, R.J. Leboeuf, Natl. Comprehensive Cancer Network 5 (2007) 641.
[16] K. Berg, H. Anholt, O. Bech, J. Moan, Brit. J. Cancer 74 (1996) 688.
[17] N.T. Le, D.R. Richardson, Biochim. Biophys. Acta 1603 (2002) 31.
[18] C.R. Chitambar, E.J. Massey, P.A. Seligman, J. Clin. Invest. 72 (1983) 1314.
[19] D.C. Yang, X.P. Jiang, R.L. Elliott, J.F. Head, Anticancer Res. 21 (2001) 1777.
[20] E.D. Harris, Nutr. Rev. 62 (2004) 60.
[21] Q. Pan, C.G. Kleer, K.L.v. Golen, Cancer Res. 62 (2002) 4854.
[22] R. Pfragner, G. Wirnsberger, B. Niederle, A. Behmel, I. Rinner, A. Mandl, F. Wawrina, J.S. Luo, D. Adamiker, H. Höger, E. Ingolic, K. Schauenstein, Int. J. Oncol. 8 (1996) 513.
[23] R. Pfragner, H. Höfler, A. Behmel, E. Ingolic, V. Walser, Cancer Res. 50 (1990) 4160.
[24] G. Stadler, M. Wieser, B. Streubel, A. Stift, J. Friedl, M. Gnant, B. Niederle, A. Beham, H. Katinger, R. Pfragner, J.M. Grillari, R. Voglauer, Eur. J. Cancer 44 (2008) 866.
[25] C. Wolf, K. Lederer, R. Pfragner, K. Schauenstein, E. Ingolic, V. Siegl, J. Mater. Sci.: Mater. Med. 18 (2007) 1247.
[26] M. Gardner, A.J. Guerin, C.A. Hunter, U. Michelsen, C. Rotger, New J. Chem. 23 (1999) 309.